Air Quality, Atmosphere & Health (2021) 14:1375–1391
https://doi.org/10.1007/s11869-021-01028-4

Exposure levels and health risk of PAHs associated with fine and ultrafine aerosols in an urban site in northern Algeria

Amira Teffahi[1] · Yacine Kerchich[1] · Yacine Moussaoui[2] · Paola Romagnoli[3] · Catia Balducci[3] · Cedric Malherbe[4] · Rabah Kerbachi[1] · Gauthier Eppe[4] · Angelo Cecinato[3,5]

Received: 17 November 2020 / Accepted: 8 April 2021 / Published online: 16 April 2021

Abstract

Size distribution of toxicants in airborne particulates remains insufficiently investigated in Algeria. A 1-year campaign was performed at Bab Ezzouar, Algiers (Algeria), aimed at characterizing particulates for their physical and chemical features. For this purpose, scanning electronic microscopy (SEM), Raman spectroscopy (RaS), and GC-MS methodologies were applied. The samples were collected on daily basis by means of a high-volume sampling (HVS) system equipped with cascade impactor separating three size fractions, i.e., particles with aerodynamic diameters d < 1.0 μm (PM_1), 1.0 μm <d<2.5 μm ($PM_{2.5}$), and 2.5 μm <d<10 μm (PM_{10}), respectively. The organic fraction was recovered from substrate through solvent extraction in an ultrasonic bath, separated and purified by column chromatography, then analyzed by gas chromatography coupled with mass spectrometry (GC-MS). Investigation was focused on polycyclic aromatic hydrocarbons (PAHs) and the concentration ratios suitable to investigate the source nature. Further information was drawn from SEM and Raman analyses. Total PAH concentrations ranged broadly throughout the study period (namely, from 4.1 to 59.7 ng m^{-3} for PM_1, from 2.72 to 32.3 ng m^{-3} for $PM_{2.5}$ and from 3.30 to 32.7 ng m^{-3} for PM_{10}). Both approaches and principal component analysis (PCA) of data revealed that emission from vehicles was the most important PAH source, while tobacco smoke provided an additional contribution.

Keywords Airborne particulate, · Polycyclic aromatic hydrocarbons (PAHs), · PAH diagnostic ratios, · Principal component analysis (PCA), · Health risk, · Algeria

Introduction

Air quality degradation is one of the important consequences of rapid industrialization and urbanization, particularly in developing countries. Consequently, in the last few years, air quality has become a subject of health and environmental concern around the world (Gadi et al. 2018).

Fine particulate matter (PM) is listed among the principal indicators of air quality. In Algeria, the annual exposure to fine particles (PM_1+$PM_{2.5}$) was about 39 μg m^{-3} (WB 2017). This value is four times higher than the standard value of 10 μg m^{-3} set by the World Health Organization (WHO). Fine particles present, at the same time, a serious risk due to small size, which helps them to reach the deeper respiratory ways and settle in the lungs (WB 2017).

Organic particulate is released by both biogenic and anthropogenic sources, i.e., living organisms and human activities, respectively (Stephanou and Stratigakis 1993). Biogenic sources include the direct suspension of pollen, micro-organisms, insects, and fragments of epicuticular waxes of vascular plants; on the other hand, man-made sources comprise the combustion of fossil fuels, industrial and house activities, agricultural debris, and wood burning (Kadowaki 1994).

Among the components of particulate organic matter (POM), polycyclic aromatic hydrocarbons (PAHs) are of

Research data related to this submission This study presents, for the first time in Algeria, the levels and sources of PAH-associated air pollution in metropolitan area of Algiers were determined, as well as PAH distribution in the three main airborne particulate size fractions.

✉ Amira Teffahi
amira.teffahi@g.enp.edu.dz

1 Laboratory of Sciences and Techniques of Environment, National Polytechnic School, El-Harrach, BP 132 Algiers, Algeria

2 Faculté des Mathématiques et Sciences de la Matière, Université Kasdi Merbah (UKMO), Ouargla, Algeria

3 Institute of Atmospheric Pollution Research (CNR-IIA), National Research Council of Italy, Via Salaria Km 29.3, Monterotondo Scalo, P.O. Box 10, 00015 Rome, Italy

4 CART, Mass Spectrometry Laboratory, UR MolSys, University of Liège, B4000, Liège, Belgium

5 Dept. of Chemistry, University "Sapienza – Roma 1", Rome, Italy

great concern, due to their ascertained carcinogenic and mutagenic potency. The four primary sources of airborne PAHs are motor vehicles (mobile: diesel and gasoline engine exhausts), home emissions, manufacturing (stationary: steel and power plants), and emissions from forest, agricultural burning and uncontrolled waste incineration. The toxicity of PAHs has been demonstrated conclusively by assays on bacterial and human cells (Mukherji et al. 2002). Besides, PAHs are direct precursors of oxy- and nitro-PAHs, the latter resulting up to 10 times more carcinogenic and 10E5 times more mutagenic than the corresponding native compounds (Durant et al. 1996).

The emission sources of organic particles can be identified by using many analytical techniques and statistical methods, the former including high-performance liquid chromatography (Eisenberg 1978) and gas chromatography coupled to mass spectrometry (Cautreels and Van Cauwenberghe 1976) applied to solvent-extractable components, and surface characterization of particles (i.e., morphology) through SEM and RaS (Bharti et al. 2017). According to literature, the spherical shape matches soot particles associated with fuel combustion, which highlights the influence of road traffic (Huda et al. 2018; Talbi et al. 2018).

On the other hand, PCA is the most used statistical approach for dimensional reduction of source matrix. PCA converts a high number of features of the original data set by using projection into few non-correlated features. Previous PCA studies undertaken in Algeria on fine particulates identified five principal emission sources of organic compounds such as alkanes, PAHs, and phthalates, namely vehicles, plastic burning, biomass burning, cooking, and mixed sources (Gadi et al. 2019).

Until today, airborne particulates have been studied in various regions of Algeria, including cities (Yassaa et al. 2001b; Ladji et al. 2009a; Moussaoui et al. 2010; Kerchich et al. 2016; Talbi et al. 2018), rural areas (Moussaoui et al. 2010), and forests (Ladji et al. 2009b; Moussaoui et al. 2013a; Khedidji et al. 2017). Both organic carbon and extractible organic matter such as n-alkanes, PAHs, nitro-PAHs, organic acids, and polar compounds were studied (Yassaa et al. 2001a, 2001c, 2001d; Moussaoui et al. 2013b). In addition, the distribution of organic solvent particulate matter was shortly investigated in ultra-fine size (PM_1) and coarse fraction (PM_{10}) at urban and forest areas (Ladji et al. 2009b), but no study has been reported for organic solvent particulate matter of fine size ($PM_{2.5}$), nor studies were conducted over one whole year. This gap was partly resolved with this study, focused on PAH assessment in PM_1, $PM_{2.5}$, and PM_{10} at Bab Ezzouar, Algiers, combined with PM characterization by means of scanning electron microscopy (SEM) and Raman spectroscopy (RaS).

Materials and methods

Study area

For our experiments, atmospheric particulates were collected over the terrace of the Medical-Social Center of Civil Protection (ca. 5 m over soil) at Bab Ezzouar city, Algiers (36° 43′ 00″ N, 3° 11′ 00″ E, see Fig. 1). Bab Ezzouar city is one of Algiers' fastest-growing municipalities, characterized by a high population density (12,045 inhabitants/km^2; NOS 2008). It includes many hotels and malls. The city is served by the Algiers train and tramway lines, the former having a station near to collection point (<100 m). Moreover, Bab Ezzouar lies very close to the Algiers international airport, and includes one of the largest universities in Africa, University of Science and Technology Houary Boumedienne of Bab Ezzouar, USTHB. Moreover, the study area is surrounded by many industrial districts, such us the Oued Smar and Dar El Beida. Finally, the sampling site is characterized by huge road traffic.

Meteorological data records were obtained from the weather station DAAG (36° 68' N, 3° 25' E), located at Dar El Beida, approximately 2 km from our study site (NOM 2019). The meteorological data included wind speed, relative humidity, and temperature (Table 1). Several studies have shown the influence of meteorological conditions on the characteristics and dispersion of fine particles. In this study, specific meteorological factors were chosen, including wind speed, relative humidity and temperature, as wind data can be used to determine the area of emissions and identify the source of pollutants. Temperature, solar radiation, and relative humidity play an important role in many chemical and photochemical reactions in the atmosphere. High and low temperature are linked with intensive and decreased convection of pollutants respectively which resulting in increased concentrations of particles in the atmosphere. In addition, higher rates of RH lead to higher PM concentrations, so air pollution events such as thermal inversion and days with high pollutant concentrations can be predicted. Meteorological parameters were studied in order to investigate seasonal variations in PM (Deng et al. 2012).

Sampling period and methodology

Particles were collected daily in three fractions on glass fiber filters (GFF, Whatman) of different sizes (20.3 × 25.4 cm^2 for PM_1 and 10 × 12 cm^2 for $PM_{2.5}$ and PM_{10}) using a HVS (Model VFC, Anderson, USA) with a PM_{10} head equipped with a cascade impactor. The sampling period lasted one year from January 2018 to January 2019. Particles had collected over 24-h intervals at the 1.1

Fig. 1 Map of sampling site

$m^3.min^{-1}$ flow rate. The fiber filters had previously backed in a chamber at constant temperature and relative humidity. Each filter was enveloped in aluminum foil (USEPA-Method IO-3.1 1999). The glass fiber filters used for particulate matter collection had weighted before and after sampling at the same percentage relative humidity (RH). The PM-enriched filters were enveloped aluminum foils and stored at a low temperature (4 °C) until analysis to preserve analytes from decomposition.

Extraction and cleanup of PAHs

Before analysis, the samples were fortified with an internal standard solution of perdeuterated homologues of analytes, used as reference compounds for quantification. The standard solution contained fluoranthene, phenanthrene, chrysene, benzo(a)anthracene, benzo(a)pyrene, perylene, benzo(ghi)perylene, and dibenz(a,h)anthracene. Filters were extracted three times for 20 min in an ultrasonic bath using a mixture of dichloromethane, acetone, and methanol (45:45:10 % v/v).

The extract was first evaporated under a gentle stream of nitrogen and purified by liquid chromatography on a neutral alumina column (6 g, deactivated with 2.5% water), then PAHs were recovered through elution with dichloromethane:isooctane (40:60 in volume, 15 mL); the eluate was reduced close to dryness under nitrogen, dissolved with toluene and analyzed by GC-MS.

Table 1 Meteorological data for the year 2018

Month	T_{max}(°C)	T_{min}(°C)	T_{ave}(°C)	Relative humidity (%)	Wind speed (km h^{-1})
Jan.18	24	02	11.4	75.9	09.0
Feb.18	26	00	10.2	77.0	10.5
Mar.18	29	02	14.0	72.8	14.2
Apr.18	29	04	16.0	74.5	11.5
May.18	33	05	17.5	79.2	10.1
Jul.18	36	15	26.2	65.3	10.8
Aug.18	37	16.5	26.5	67.5	10.2
Sep.18	36	16	24.6	72.2	10.0
Oct.18	33	08	19.7	71.6	10.2
Nov.18	28	03	15.7	71.2	10.6
Dec.18	25	02	11.9	81.6	06.6
Jan.19	20	00	09.9	79.0	10.9

GC/MS analysis

Individual PAHs were characterized using a gas chromatograph equipped with a mass spectrometer (Trace-GC and Trace Q MS) and controlled by the proprietary software Excalibur (all from Thermo Fisher, Rodano MI, Italy). The analytes were separated applying a temperature gradient from 90 up to 290°C to a 25-m-long RT5MS type column (i.d. = 250 μm, film thickness = 0.33 μm, Superchrom, Milan, Italy), under a Helium constant flow of 1.0 $mL.min^{-1}$. For identification, the combination of relative retention times, mass spectra and ion trace ratios of the peaks was compared with that of authentic PAH standards. For quantitative purposes, the peak area of each compound had compared with that of its perdeuterated homologue or the closest internal reference in the chromatogram (isotopic dilution method). The quantitative data were kept as reliable when the resulting concentrations lied within the operating ranges of the detector, i.e., 3.3 to ~ 1000 times the respective detection limits.

Filter blanks were included in the chromatograms in the correspondence; in the cases of phenanthrene and pyrene (light PAH congeners), blanks were quite important and accounted for in the quantitative determinations. The recovery rates varied between 83% and 106% (±9%), and the accuracy was better than 11% for all species.

Scanning electronic microscopy (SEM) analysis

In order to recognize the morphology of the three fractions of airborne particles, the samples were processed by SEM (JEOL, JSM-6360). For this purpose, portions of 1.0 cm^2 were cut from each particulate-loaded filter and attached to aluminum holders with double-sided adhesive carbon tape. To make the surface conductive, they were covered with a very thin film of gold using a vacuum coating unit (Cressington, Carbon Coater 108 carbon / A). Samples were examined and photographs taken at different magnifications using an accelerating voltage of 25 kV and 30 tilt stereo SEM.

Raman spectroscopy (RaS) analysis

The three particle fractions (PM_{10}, $PM_{2.5}$, and PM_1) were analyzed using a LabRam 300 spectrometer (Jobin-Yvon) featuring an Olympus confocal microscope and an Andor BRDD Du401 CCD detector. According to the color of the particle, two different objectives (×50 or ×100 magnification) had adopted.

The maximum powers of the induced beam laser on the sample were 5 mW (green laser) and 30 mW (red laser). From one sample to another, the integration times were between 5 s and 50 s. Two spectral databases were used for matching, i.e., a personal library, which used Thermo Spectra 2.0 software, and a commercially available database (OmnicSpectra software, Thermo Fisher Scientific, USA).

Results and discussion

SEM analysis

The results of SEM indicated a variety of particle shapes and sizes; the morphology of the particles studied was widely variable and corresponded to irregular, aggregate, spherical, or spheroidal shapes (Fig. 2). Three types of particulate matter were observed, i.e., soot, inorganic compounds, tar balls, in addition to the fourth group of non-identified particles. The shape and size of the particles changed according to their way of formation and distance from the source. For instance, the aggregated and spherical shapes that refer to soot particles generated by fuel combustion showed the impact of road traffic on the sampling site, while the coarser particles had the tendency to approach the source. According to studies previously published dealing with particle morphology, irregular and spherical shapes refer to inorganic compounds and tar balls, respectively (Cong et al. 2010; Bharti et al. 2017; Talbi et al. 2018).

RaS analysis

Analyses, carried out on three particle fractions (PM_{10}, $PM_{2.5}$, and PM_1), showed the presence of a number of bands linked to metal oxides, sulfates, and organic compounds. Table 2 illustrates a summary of the molecular composition of the characterized PM.

Figure 3 shows characteristic Raman spectra of PM_{10}, $PM_{2.5}$, and PM_1, samples. All of them were characterized by pronounced peaks at ~1350 cm^{-1} and ~1600 cm^{-1}. Both identified bands were identical to those of standard graphite, in particular activated carbon, as well as to bands typical of inorganic compounds. A small peak at 470 cm^{-1}, probably quartz, a large peak between 600 and 800 cm^{-1}, attributed to hematite Fe_2O_3, the peaks at 420 and 1008 cm^{-1}, indicating the existence of gypsum ($CaSO_4$•$2H_2O$), and finally the peak at 1000 cm^{-1}, possibly associated with celestine ($SrSO_4$) as representative of sulfate mixture, were also observed.

Particulate matter mass concentration

Particulate matter size distribution

As shown in Fig. 4, the daily mass concentrations of PM_{10}, $PM_{2.5}$, and PM_1 ranged from 22.6 to 260 μg m^{-3}, from 12.7 to 180 μg m^{-3}, and from 8.7 to155 μg m^{-3}, respectively. The daily evolution of particulate matter reveals important fluctuations for all the three size fractions, with standard deviations

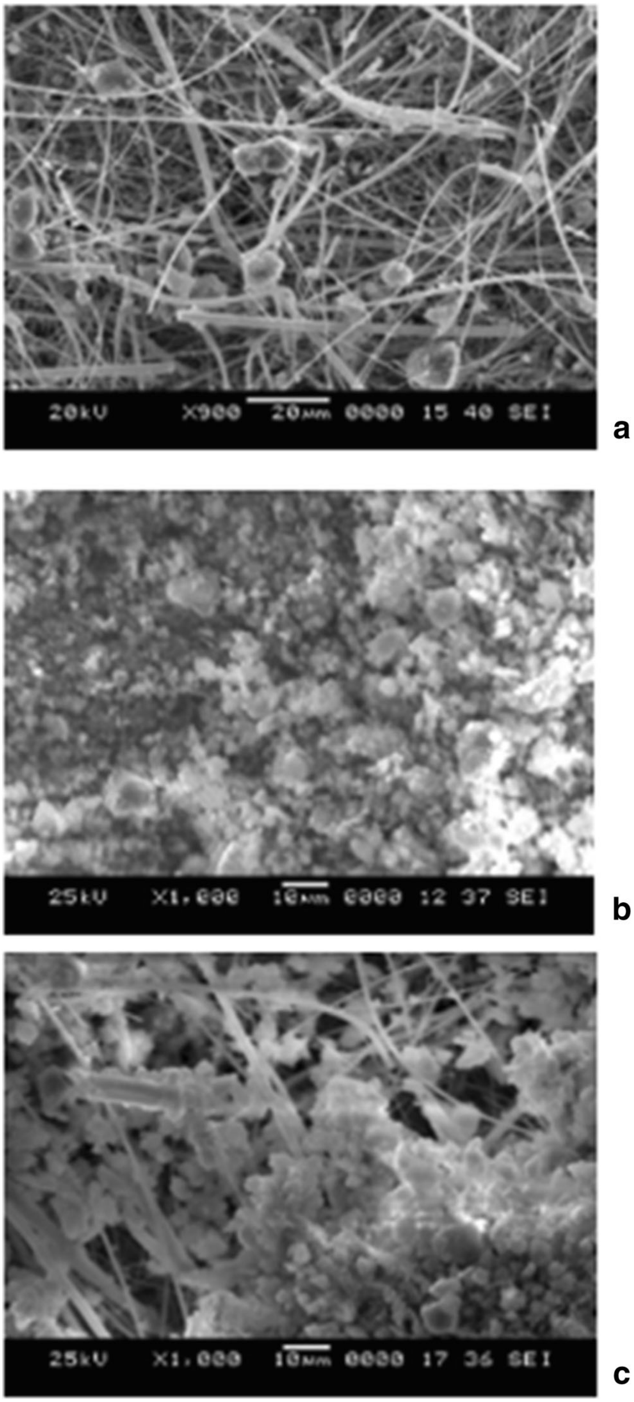

Fig. 2 SEM images of lodes filter in: A= PM_1, B= $PM_{2.5}$, C= PM_{10}

as high as 39.4 µg m^{-3}, 25.2 µg m^{-3}, and 21.6 µg m^3, respectively, for PM_{10}, $PM_{2.5}$, and PM_1. The concentrations of PM_{10} and $PM_{2.5}$ respectively is about 93% and 91% of days during 1 year of campaigne were greater than WHO Guidelines, which indicates that the population is exposed to high levels of fine particle pollution.

Two tests were performed with the statistical software R which are Student's tests *t*-test and Mann-Whitney *U*-tests (MWU) to compare the data sets and determine if they

Table 2 Molecular composition of the characterized PM

Analyzed particles	Particle name	Raman bands (cm^{-1})
SiO_2	Quartz	470 cm^{-1}
Fe_2O_3	Hematite	600–800 cm^{-1}
C	Carbone	1300 cm^{-1} and 1600 cm^{-1}
$CaCO_3$	Calcite	749 cm^{-1} et 1086 cm^{-1}
TiO_2	Rutile	647 cm^{-1}
$CaSO_4.2H_2O$	Gypsum	420 cm^{-1} and 1008 cm^{-1}
$SrSO_4$	Celestine	1000 cm^{-1}

were statistically different from each other. Both tests were performed with a significance level of 0.05 (95% confidence).

Paired-Student *t*-tests were performed between paired measurements (PM_{10} and PM_1, PM_{10} and $PM_{2.5}$, $PM_{2.5}$, and PM_1). The *p*-values were $< 2.2 \times 10^{-16}$ for all paired measurements, the mean value of the difference was 48.50 for PM_{10} and $PM_{2.5}$, 15.15 for $PM_{2.5}$ and PM_1 and 63.64 for PM_{10} and PM_1. The results showed that the mean difference between paired measurements is significant different, this result is confirmed by *U*-test ($P < 10^{-14}$) with a p value < 0.05 indicating significant differences between the paired measurements.

The monthly average mass concentrations varied from 68 to 140 µg m^{-3}, 30–76 µg m^{-3}, and from 16.6–56 µg m^{-3}, respectively, for PM_{10}, $PM_{2.5}$, and PM_1 (Fig. 5). The *p*-values of *t*-test were $< 1.21 \times 10^{-7}$ for PM_{10} and $PM_{2.5}$, the same value for PM_1 and $PM_{2.5}$ and 8.47×10^{-8} for PM_{10} and PM_1, the mean value of the difference was 49.33 for PM_{10} and $PM_{2.5}$, 15.62 for $PM_{2.5}$ and PM_1 and 64.94 for PM_{10} and

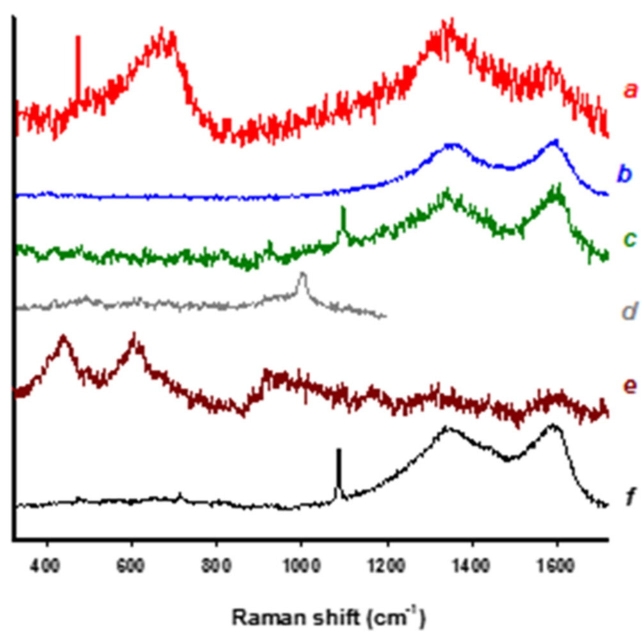

Fig. 3 Raman spectra of PM_{10}, $PM_{2.5}$, and PM_1: (a) quartz and hematite; (b) carbone; (c) calcite; (d) sulfate; (e) rutile; (f) gypsum; and celestine

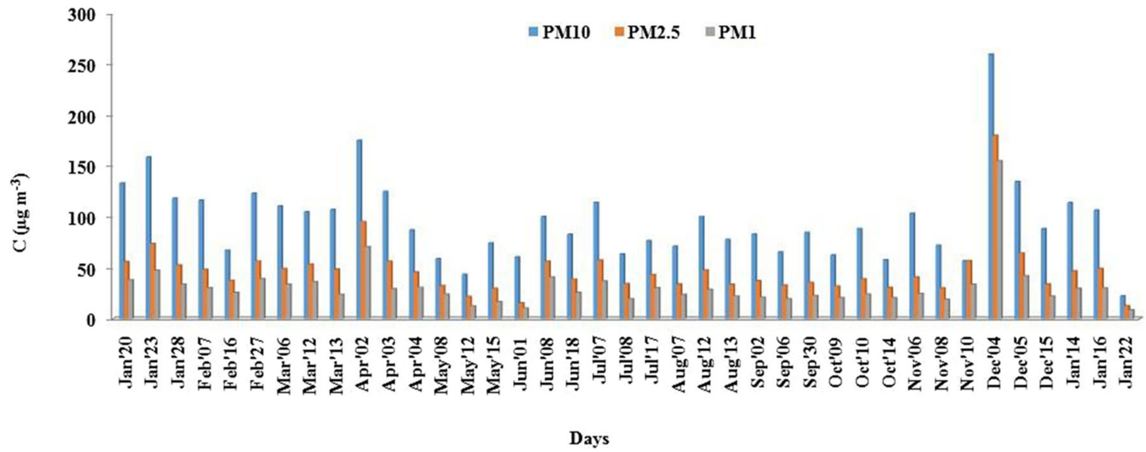

Fig. 4 Daily evolution of PM concentrations at study area

PM_1. Two main factors seemed to influence the time fluctuations of SPM (Suspend Particulate Matter), i.e., the daily road traffic rate and weather. Indeed, the maximum concentration was recorded in December; this can be explained by the combination of various sources, in particular the extension of the Algiers metro line up to 100 m away from the sampling site and unfavorable weather conditions (this month was characterized by weak wind speeds and high humidity).

The annual average of mass concentrations reached 94.8 ± 11.4 µg m^{-3} for PM_{10}, 46.3± 7.3 µg m^{-3} for $PM_{2.5}$, and 31.1± 6.4 µg m^{-3} for PM_1. Therefore, all of the annual average limits of 80 µg m^{-3}, 40 µg m^{-3}, and 20 µg m^{-3} fixed for PM_{10} by the Algerian air quality standard, the EU Air Quality Directive, and the WHO guidelines, respectively, were exceeded. Besides, the three fractions cumulatively reached 169 µg m^{-3} as yearly average (119–272 µg m^{-3}, σ = 47 µg m^{-3}), which means over 3 times the limit established by European normative (European Union 2008) to preserve human health. As for $PM_{2.5}$, the mean concentration was over four times higher than the WHO guideline. This level of pollution appears as a cause for health concern, overall because of the strong presence of very fine particles, where PM_1 represents ca 1/3 of PM_{10}.

The weather in Algiers is of Mediterranean type characterized by hot and dry summers, wet and cool winters.

Figure 6 presents the seasonal mean profiles of PM_{10}, $PM_{2.5}$, and PM_1. A weak seasonal fluctuation was observed for $PM_{2.5}$ and PM_1; by contrast, an important seasonal behavior had found for PM_{10}. As pictured in Fig. 6, the highest concentrations were typically found in the winter, may be associated with important factors that promote the accumulation of particles in the atmosphere and limit particle dispersion, i.e., combustion of fossil fuels and coal, resuspension of road dust and a shallower mixing layer, while the lowest concentrations were detected in the autumn. These low concentrations are probably due to the winds formed during the heat exchanges that occur between cold air masses and warm air masses during the fall. This season is particularly marked by frequent windy and rainy weather, resulting in good dispersion of pollutants.

The annual mean concentrations of PM_{10} were in agreement with those resulting from previous studies conducted in

Fig. 5 Monthly evolution of PM concentrations at study area

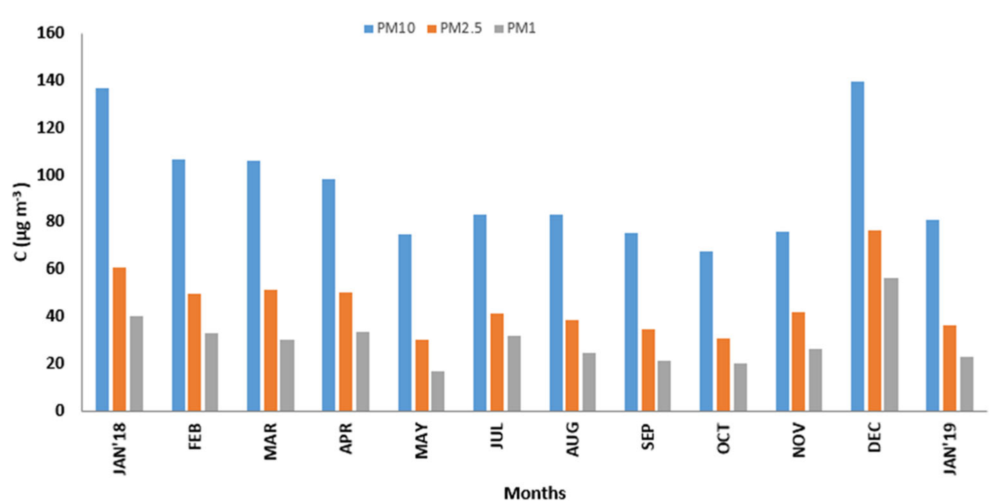

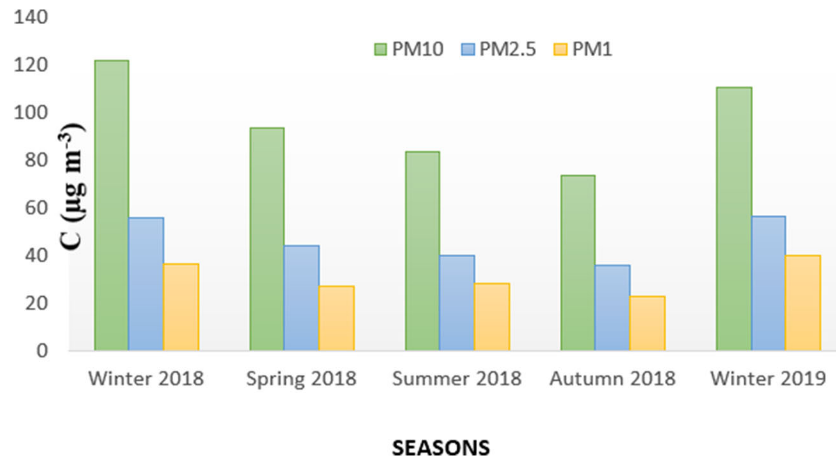

Fig. 6 Seasonal mean profiles of PM_{10}, $PM_{2.5}$, and PM_1

Algeria (Oucher and Kerbachi 2012; Terrouche and Ali-khodja 2015; Talbi et al. 2018); at the same time, they exceeded those observed in European countries (WHO 2014), e.g., in Spain, Italy, and Portugal (varied between 22 and 40 µg m^{-3}), but were lesser than those of countries known for their high pollution rates, such as United Arab Emirates (160 µg m^{-3}), Palestine (175 µg m^{-3}), and Egypt (108–450 µg m^{-3}) (Jodeh et al. 2018; Zahran et al. 2018).

Similarities existed among the levels of $PM_{2.5}$ found in this study and those reported from India (46 µg m^{-3}) and Turkey (43 µg m^{-3}) (WHO 2014), but our rates were higher than those detected in Malaysia and Brazil (28 and 11 µg m^{-3}, respectively; Amil et al. 2016; Franzin et al. 2020), and lower than those of China (56 µg m^{-3} ; Chen et al. 2017). The concentrations of $PM_{2.5}$ in the megacities Delhi in India during the CoViD-19 lockdown were as high as 38 µg m^{-3} (ca 52 µg m^{-3} off from normal situation). According to that, it is expected that also in Bab Ezzouar pollution was reduced during pandemic period (Mahato et al. 2020).

The measured concentrations of PM_1 (31.1± 6.4 µg m^{-3}) are higher than those reported from Czech Republic (17 µg m^{-3}) (Kozáková et al. 2018) and Poland (14 µg m^{-3}) (Rogula-Kozłowska et al. 2019) in the urban area.

Statistical parameters of the particulate matter studied

Table 3 presents the Pearson correlations between the mean concentrations of airborne particles and mean meteorological factors. Throughout the study, a p-value of <0.05 was regarded as statistically significant. The resulting correlations rates were poor, pointing out that no relationship existed between atmospheric particle concentrations and temperature, relative humidity, and wind speed. A possible explanation for this is the short distance from the sampling site to road traffic (<5 m), which means that the influence of meteorological conditions on the PM is barely visible.

Table 3 Pearson correlations between PM and meteorological factors

	T	V	RH
PM_1	0.39 (r^2 =0.0761)	0.17 (r^2 =0.1808)	0.69 (r^2 =0.0161)
$PM_{2.5}$	0.24 (r^2 =0.1355)	0.31 (r^2 =0.1041)	0.53 (r^2 =0.0398)
PM_{10}	0.1 (r^2 =0.2447)	0.22 (r^2 =0.1439)	0.28 (r^2 =0.1177)

T average temperature (°C), *V* average wind speed (Km h^{-1}), *RH* average relative humidity (%)

On the other hand, the correlation coefficients between the next respective pairs of PM fractions, i.e., PM_{10}–$PM_{2.5}$ (p = 2.22.10^{-6}), PM_{10}–PM_1 ($p = 2.14 \times 10^{-4}$), and $PM_{2.5}$–PM_1 (p = 1.05×10^{-6}) indicate meaningful correlations among all fractions. These findings are in accordance with previous researches carried out in Algiers (Talbi et al. 2018).

The PM_1/PM_{10}, $PM_1/PM_{2.5}$, and $PM_{2.5}/PM_{10}$ ratios are shown in Fig. 7. The annual averages recorded in this study were 0.29, 0.63, and 0.46, respectively, for PM_1/PM_{10}, $PM_1/PM_{2.5}$, and $PM_{2.5}/PM_{10}$; hence, in the average PM_1, $PM_{2.5}$, and PM_{10} accounted for 21%, 29%, and 60% of the total (SPM = PM_1+$PM_{2.5}$+PM_{10}) over the whole year. The PM_1/PM_{10}, $PM_1/PM_{2.5}$, and $PM_{2.5}/PM_{10}$ ratios were analogous to those previously found in Algiers, i.e., 0.30, 0.58, and 0.51, respectively (Talbi et al. 2018). The ratio $PM_{2.5}/PM_{10}$ ratio was about 0.5, indicating that coarse particles from road dust

Fig. 7 Annual averages of PM1/PM10, PM1/PM2.5, and PM2.5/PM10

Table 4 Concentration of PAHs identified in PM_{10} from January 2018 for January 2019

Compounds	Abbreviation	Unit	01/18	02/18	03/18	04/18	05/18	07/18	08/18	09/18	10/18	11/18	12/18	01/19
PM	PM_{10}	$\mu g\ m^{-3}$	137.08	106.56	106.22	98.21	74.81	83.27	83.37	75.42	67.86	75.95	139.67	81.18
Phenanthrene	PHE	$ng\ m^{-3}$	0.51	0.12	0.09	0.14	0.06	0.1	0.19	0.09	0.1	0.09	0.28	0.18
Anthracene	AN	$ng\ m^{-3}$	0.04	0.01	0.01	0.02	0.01	0.01	0.02	0.01	0.01	0.01	0.04	0.02
methyl Phenanthrene/anthracene	MeP/A	$ng\ m^{-3}$	0.49	0.17	0.17	0.24	0.1	0.13	0.19	0.12	0.13	0.12	0.36	0.21
dimethyl-Phenanthrene/anthracene	DMeP/A	$ng\ m^{-3}$	0.39	0.2	0.26	0.29	0.11	0.2	0.19	0.18	0.15	0.18	0.51	0.33
Fluoranthene	FA	$ng\ m^{-3}$	0.3	0.11	0.08	0.1	0.04	0.07	0.13	0.09	0.12	0.1	0.35	0.23
Pyrene	PY	$ng\ m^{-3}$	0.32	0.12	0.09	0.13	0.04	0.08	0.13	0.09	0.13	0.12	0.48	0.26
Methyl-Fluoranthene/pyrene	MeF/P	$ng\ m^{-3}$	0.29	0.11	0.08	0.12	0.05	0.06	0.15	0.07	0.08	0.1	0.52	0.23
Benzo(ghi)fluoranthene	BghiF	$ng\ m^{-3}$	0.49	0.45	0.11	0.16	0.04	0.05	0.08	0.07	0.09	0.12	0.76	0.31
Benzo(c)phenanthrene	BcP	$ng\ m^{-3}$	0.08	0.06	0.02	0.02	0.01	0.01	0.01	0.01	0.01	0.02	0.12	0.05
Cyclopenta(c,d)pyrene	CPP	$ng\ m^{-3}$	0.19	0.07	0.04	0.08	0.01	0.03	0.05	0.03	0.05	0.05	0.49	0.21
Benz[a]anthracene	BaA	$ng\ m^{-3}$	0.51	0.14	0.09	0.14	0.04	0.05	0.09	0.06	0.06	0.12	0.99	0.35
Chrysene+trifenilene	CH+TR	$ng\ m^{-3}$	1.4	0.62	0.34	0.46	0.18	0.17	0.27	0.25	0.23	0.35	2.2	0.79
Benzo[b]fluoranthen	BbF	$ng\ m^{-3}$	2.61	1.3	0.55	0.83	0.25	0.39	0.54	0.42	0.41	0.57	3.09	1.49
Benzo[j,k]fluoranthene	BjkF	$ng\ m^{-3}$	2.94	0.91	0.7	1.01	0.37	0.52	0.68	0.56	0.54	0.71	3.48	1.78
Benzo[e]pyrene	BeP	$ng\ m^{-3}$	3.35	2.54	0.77	1.04	0.32	0.58	0.79	0.55	0.57	0.68	3.37	1.75
Benzo[a]pyrene	BaP	$ng\ m^{-3}$	1.64	0.47	0.26	0.42	0.09	0.16	0.24	0.14	0.17	0.21	2.2	1.15
Perylene	PE	$ng\ m^{-3}$	0.28	0.13	0.05	0.08	0.02	0.03	0.04	0.02	0.03	0.03	0.36	0.19
Indeno[1.2.3-cd]pyrene	IP	$ng\ m^{-3}$	3.87	1.25	1.21	1.72	0.48	0.86	1.12	0.79	0.79	0.89	4.53	2.84
Benzo[ghi]perylene	BPE	$ng\ m^{-3}$	6.9	5.25	2.67	3.99	0.97	1.71	2.29	1.61	1.75	1.87	7.82	4.59
Dibenz[a.h]anthracene	DBahA	$ng\ m^{-3}$	0.63	0.15	0.19	0.23	0.16	0.15	0.19	0.12	0.11	0.12	0.71	0.4
Total PAHs		$\mathbf{ng\ m^{-3}}$	**27.2**	**14.2**	**7.8**	**11.2**	**3.3**	**5.4**	**7.4**	**5.3**	**5.5**	**12.1**	**32.7**	**17.4**

Table 5 Concentration of PAHs identified in $PM_{2.5}$ from January 2018 for January 2019

Compounds	Abbreviation	Unit	01/18	02/18	03/18	04/18	05/18	07/18	08/18	09/18	10/18	11/18	12/18	01/19
PM	$PM_{2.5}$	$\mu g\ m^{-3}$	61.17	49.58	51.20	50.50	29.99	41.55	38.47	34.42	30.86	41.72	76.37	36.42
Phenanthrene	PHE	$ng\ m^{-3}$	0.37	0.09	0.07	0.11	0.04	0.08	0.15	0.07	0.08	0.07	0.24	0.16
Anthracene	AN	$ng\ m^{-3}$	0.03	0.01	0.01	0.02	0	0.01	0.01	0	0.01	0.01	0.04	0.02
methyl-Phenanthrene/anthracene	MeP/A	$ng\ m^{-3}$	0.35	0.12	0.12	0.19	0.07	0.11	0.15	0.09	0.1	0.09	0.28	0.18
dimethyl-Phenanthrene/anthracene	DMeP/A	$ng\ m^{-3}$	0.39	0.2	0.18	0.29	0.11	0.16	0.19	0.13	0.15	0.12	0.39	0.27
Fluoranthene	FA	$ng\ m^{-3}$	0.24	0.09	0.06	0.08	0.03	0.06	0.1	0.07	0.09	0.07	0.29	0.21
Pyrene	PY	$ng\ m^{-3}$	0.26	0.1	0.07	0.12	0.03	0.07	0.11	0.07	0.11	0.09	0.41	0.23
methyl-Fluoranthene/pyrene	MeF/P	$ng\ m^{-3}$	0.23	0.08	0.06	0.1	0.04	0.05	0.07	0.06	0.07	0.07	0.41	0.19
Benzo(ghi)fluoranthene	BghiF	$ng\ m^{-3}$	0.35	0.14	0.08	0.13	0.03	0.04	0.07	0.06	0.07	0.09	0.6	0.27
Benzo(c)phenanthrene	BcP	$ng\ m^{-3}$	0.06	0.02	0.01	0.02	0.01	0.01	0.01	0.01	0.01	0.01	0.1	0.04
Cyclopenta(c,d)pyrene	CPP	$ng\ m^{-3}$	0.17	0.05	0.04	0.08	0.01	0.03	0.05	0.03	0.05	0.04	0.44	0.2
Benz[a]anthracene	BaA	$ng\ m^{-3}$	0.39	0.11	0.07	0.12	0.03	0.04	0.08	0.05	0.05	0.09	0.79	0.31
Chrysene+trifenilene	CH+TR	$ng\ m^{-3}$	0.97	0.35	0.23	0.37	0.13	0.15	0.22	0.2	0.18	0.24	1.71	0.68
Benzo[b]fluoranthen	BbF	$ng\ m^{-3}$	1.97	1.02	0.43	0.71	0.18	0.34	0.48	0.34	0.35	0.45	2.55	1.35
Benzo[j,k]fluoranthene	BjkF	$ng\ m^{-3}$	2.1	0.51	0.51	0.84	0.27	0.45	0.58	0.45	0.43	0.57	2.79	1.59
Benzo[e]pyrene	BeP	$ng\ m^{-3}$	2.51	2.13	0.57	0.87	0.23	0.5	0.65	0.44	0.45	0.54	2.84	1.59
Benzo[a]pyrene	BaP	$ng\ m^{-3}$	1.33	0.36	0.22	0.38	0.08	0.15	0.23	0.12	0.15	0.18	1.93	1.08
Perylene	PE	$ng\ m^{-3}$	0.22	0.11	0.04	0.07	0.01	0.03	0.04	0.02	0.02	0.03	0.32	0.18
Indeno[1.2.3-cd]pyrene	IP	$ng\ m^{-3}$	3.5	1.07	1.12	1.58	0.43	0.82	1.03	0.69	0.72	0.81	4.24	2.71
Benzo[ghi]perylene	BPE	$ng\ m^{-3}$	6.2	4.85	2.45	3.64	0.84	1.62	2.01	1.39	1.57	1.68	7.29	4.35
Dibenz[a.h]anthracene	DBahA	$ng\ m^{-3}$	0.56	0.12	0.17	0.21	0.14	0.14	0.17	0.11	0.1	0.1	0.66	0.38
Total PAHs		**$ng\ m^{-3}$**	**22.21**	**11.52**	**6.51**	**9.95**	**2.72**	**4.88**	**6.39**	**4.39**	**4.77**	**5.37**	**28.33**	**16.02**

resuspension and abrasion processes are the dominant fraction of the particulates.

PAHs

GC/MS analysis

Twenty PAHs had identified and quantified in PM_{10}, $PM_{2.5}$, and PM_1 (Tables 4, 5, 6). The mean concentration of individual PAHs ranged from 0.02± 0.01 to 3.45± 1.27 ng m^{-3}, from 0.01± 0.006 to 3.16± 1.19 ng m^{-3}, and from 0.04± 0.003 to 7.88± 2.63 ng m^{-3} for PM_{10}, $PM_{2.5}$, and PM_1, respectively. The most volatile among the 20 PAHs analyzed (Fig. 8), namely naphthalene, acenaphthene, and fluorene, were not detected in airborne particles, because the 2/3-ring aromatic molecules occur predominantly in the gaseous phase of atmosphere, at ambient temperatures typical of North Western Africa. The results are in accordance with other studies conducted in that region (Jamhari et al. 2014).

The mean concentrations of total PAHs (T-PAHs) in PM_1, $PM_{2.5}$, and PM_{10} were equal to 24.9 ± 9.9 ng m^{-3} (4.1-59.7 ng m^{-3}), 10.3 ± 4.5 ng m^{-3} (2.72-28.3 ng m^{-3}), and 12.5± 5.2 ng m^{-3} (3.3-32.7 ng m^{-3}), respectively. Cumulatively, T-PAHs reached 47.6 ± 34.5 ng m^{-3}over the measurement period. As for size distribution, T-PAHs were preferably associated to PM_1 fraction (52.2 ± 5.5%), the remaining being almost equally partitioned between $PM_{2.5}$ and PM_{10} (21.3 ± 2.6% and 26.4 ± 4.6%, respectively), with minor differences among the months. The important content of PAHs in PM_1 was that typically originated by organic fuel combustion, known as producing ultrafine particles heavily affected by PAHs (Landkocz et al. 2017). Indeed, T-PAHs accounted for 790 ± 420 p.p.m. in mass of PM_1, 210 ± 120 ppm of $PM_{2.5}$ and 120 ± 60 p.p.m. of PM_{10}. Nonetheless, some monthly variability in the relative abundance of PAHs in the three fraction was observed, with percentages in PM_{10} peaking in May and November. The reasons of is behaviour are still unknown and seems to merit further investigation, though presumably related with nature of sources. As shown in Fig. 9, ~50% of T-PAHs were associated with particles <0.95 μm, and up to 90% with particles <2.5 μm. Noteworthy, PAHs accumulate mainly in the form of fine and ultrafine particles, which could pose a potential health risk. Finally, most of particulate PAHs (~88% of the total) belong to high molecular weight range (MW ≥276), however the percentage of low molecular weight PAHs (2–3 ring congeners) is relatively more abundant in the warm season ~16% July to September vs. ~9% December to February). This pattern, apparently inconsistent with ambient temperature profile that should promote the passage of PAHs into the gas phase, has been associated to emission from asphalts and uncontrolled fires (e.g., vegetation) (Cecinato et al. 2014).

The PM_{10}-bound PAH concentrations reported in our study were much lower than those previously recorded in urban areas, such as 97 to 137 ng m^{-3} in Tehran (Hoseini et al. 2016) and 14 to 420 ng m^{-3} in Alexandria, Egypt (Khairy and Lohmann 2013). The results of this study were also higher than the 2.8 ng m^{-3} recorded for Bizerte, Tunisia (Barhoumi et al. 2018) and the average of 3 ng m^{-3} in Boumerdes, Algeria (Ladji et al. 2009b) and in agreement with those recorded in Bab el Oued and Ben Aknoun (Algiers, Algeria), ranging from 8.4 ng m^{-3} to 19 ng m^{-3} (Ladji et al. 2009a).

The measured concentrations of T-PAHs for $PM_{2.5}$ and PM_1 were higher than those reported in Athens (Greece), which ranged from 0.43 to 1.56 ng m^{-3} and from 0.21 to 0.9 ng m^{-3}, respectively (Pateraki et al. 2019). On the other hand, these latter were lower than those recorded in Kigali (Rwanda), which varied from 19.3 ng m^{-3} to 54.9 ng m^{-3} for $PM_{2.5}$ (Kalisa et al. 2018), and those recorded at Porto (Brazil),which ranged from 1.32 to 3.05 ng m^{-3} for PM_1 (Agudelo-Castañeda and Teixeira 2014), and comparable with those found in Brno and Slapanice (Czech Republic), where a concentration of 22.2 ng m^{-3} was recorded in winter time in PM_1 (Krumal et al. 2013).

The average concentrations of the PM_{10}-and $PM_{2.5}$-bound class 1 carcinogen BaP were 0.60 ± 0.34 ng m^{-3} and 0.52 ± 0.29 ng m^{-3}, respectively, whereas the average in the PM_1-bound fraction was 1.26 ng m^{-3}, exceeding 1 ng m^{-3}. Cumulatively, BaP reached 2.38 ng m^{-3} and exceeded by far the EU reference value of 1 ng m^{-3} averaged over the calendar year.

The concentrations of PAHs in all three fractions were clearly higher during the cold vs. the warm season. This pattern is primarily the result of emission rate increase from year time modulated sources, like residential heating and motor vehicle traffic. In the colder months, there is also the concurrent impact of atmospheric conditions, characterized by frequent thermal inversions, low mixed layer and considerably reduced atmospheric dispersion. Conversely, the hot period experienced reduced PAH levels thanks to stop of heating plant emissions and to meteorological conditions promoting the gas-phase partition and photo-degradation of PAHs; moreover, PAH concentrations could drop due to photo-oxidation promoted by solar radiation and induced by numerous atmospheric oxidants, namely free radicals such as OH, NO_3, NO_2 and ozone (Manoli et al. 2015).

BPE and IP were the most abundant PAHs in the three fractions; according to previous studies, relatively high concentration of BPE and IP are associated with exhausts of gasoline-powered vehicles, while lower PAHs including FA, PHE, PY, and CH are overall associated to diesel-powered vehicles (Jamhari et al. 2014).

The principal PAHs in all three fractions of particulate matter were BbF, BjkF, CH, FA, IP, BeP, and BPE, which cumulatively accounted for > 80% of the T-PAHs. This seemed

Table 6 Concentration of PAHs identified in PM_1 from January 2018 for January 2019

Compounds	Abbreviation	Unit	01/18	02/18	03/18	04/18	05/18	07/18	08/18	09/18	10/18	11/18	12/18	01/19
PM	PM_1	μg m^{-3}	39.97	32.96	30.27	33.63	16.67	32.08	24.43	21.24	20.00	26.37	56.42	23.01
Phenanthrene	PHE	ng m^{-3}	0.85	0.2	0.15	0.32	0.06	0.25	0.41	0.16	0.2	0.19	0.5	0.34
Anthracene	AN	ng m^{-3}	0.05	0.05	0.05	0.05	0.05	0.05	0.05	0.05	0.05	0.02	0.05	0.05
methyl-phenanthrene/anthracene	MeP/A	ng m^{-3}	0.8	0.29	0.24	0.53	0.09	0.32	0.39	0.23	0.26	0.24	0.6	0.37
dimethyl-Phenanthrene/anthracene	DMeP/A	ng m^{-3}	0.85	0.49	0.35	0.77	0.12	0.46	0.51	0.34	0.38	0.33	0.84	0.55
Fluoranthene	FA	ng m^{-3}	0.55	0.21	0.14	0.22	0.04	0.18	0.25	0.15	0.21	0.19	0.58	0.43
Pyrene	PY	ng m^{-3}	0.62	0.25	0.17	0.34	0.04	0.22	0.29	0.18	0.28	0.26	0.91	0.5
methyl-Fluoranthene/pyrene	MeF/P	ng m^{-3}	0.53	0.22	0.13	0.29	0.05	0.15	0.18	0.14	0.18	0.18	0.81	0.43
Benzo(ghi)fluoranthene	BghiF	ng m^{-3}	0.82	0.34	0.2	0.38	0.04	0.14	0.18	0.15	0.2	0.25	1.24	0.65
Benzo(c)phenanthrene	BcP	ng m^{-3}	0.12	0.05	0.03	0.05	0.01	0.02	0.03	0.02	0.02	0.03	0.18	0.1
Cyclopenta(c,d)pyrene	CPP	ng m^{-3}	0.5	0.15	0.11	0.26	0.02	0.11	0.16	0.09	0.16	0.16	1.15	0.57
Benz[a]anthracene	BaA	ng m^{-3}	0.9	0.28	0.17	0.36	0.03	0.13	0.2	0.12	0.16	0.22	1.63	0.74
Chrysene+trifenilene	CH+TR	ng m^{-3}	2.21	0.85	0.54	1.07	0.15	0.44	0.55	0.47	0.49	0.62	3.5	1.6
Benzo[b]fluoranthen	BbF	ng m^{-3}	4.95	1.75	1.06	2.13	0.23	1.09	1.26	0.84	0.99	1.25	5.61	3.43
Benzo[j,k]fluoranthene	BjkF	ng m^{-3}	5.3	2.03	1.27	2.5	0.42	1.43	1.52	1.14	1.19	1.59	5.91	3.87
Benzo[e]pyrene	BeP	ng m^{-3}	6.06	2.22	1.36	2.53	0.32	1.52	1.76	1.11	1.28	1.52	6.04	3.88
Benzo[a]pyrene	BaP	ng m^{-3}	3.47	0.86	0.55	1.13	0.07	0.5	0.63	0.28	0.45	0.53	4.03	2.66
Perylene	PE	ng m^{-3}	0.52	0.16	0.1	0.21	0.01	0.1	0.11	0.05	0.07	0.08	0.65	0.39
Indeno[1.2.3-cd]pyrene	IP	ng m^{-3}	8.35	3.83	2.77	4.51	0.66	2.63	2.65	1.6	1.93	2.19	8.4	6.92
Benzo[ghi]perylene	BPE	ng m^{-3}	15.36	7.89	6.8	11.26	1.54	5.19	5.57	3.53	4.62	5.13	15.88	11.8
Dibenz[a.h]anthracene	DBahA	ng m^{-3}	1.18	0.47	0.38	0.53	0.17	0.41	0.39	0.21	0.25	0.26	1.16	0.89
Total PAHs		**ng m^{-3}**	**53.96**	**22.58**	**16.56**	**29.45**	**4.12**	**15.35**	**17.1**	**10.85**	**13.38**	**15.28**	**59.66**	**40.17**

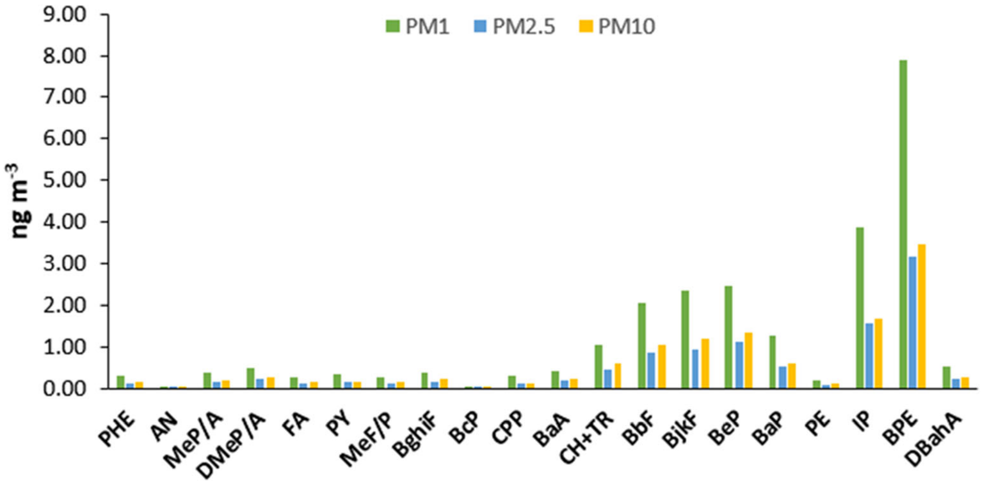

Fig. 8 Average concentrations of 20 PAHs associated with particulate matter

indicative of high impact of vehicle exhausts on air quality; indeed, BeP and BPE associated to particulate matter are used to recognize emission from gasoline- and diesel-powered engines (He et al. 2014), suggesting the presence of local pollution and low photo-degradation (Romagnoli et al. 2019).

Figure 10 presents the PAH ring number distribution in PM_{10}. According to pie chart, the contribution of high molecular weight congeners (5/6-ring PAHs) in PM_{10} is up to 88%. On the other hand, medium (4-ring) and low molecular weight PAHs (2/3-ring) accounted for 10% and 2% of the total PAHs, respectively. The high percentage of high molecular weight PAHs indicates the sources are high-temperature processes, e.g., fuel combustion in engines (Jamhari et al. 2014).

Emission source identification

PAHs diagnostic ratios PAH diagnostic ratios are a practical tool for the identification of probable sources on the basis of the concentrations of specific PAH compounds or groups and have been developed and used by a number of environmental researchers.

The values of calculated diagnostic ratios for the particulate matter studied and characteristic diagnostic ratios obtained from preceding literature are reported in Table 7. From the comparison of the diagnostic ratios shown in Table 7, the majority of the calculated diagnostic ratios were within the range of gasoline, diesel, and coal emissions.

In this study, the FA/PY, IP/BPE, BaP/BeP, and BaP/BPE ratios were equal to 0.90, 0.48, 0.37, and 0.14, respectively. According to them, diesel vehicles were the principal source of emissions. Other emission sources were identified looking to (BaP/BPE) and (BaP/BeP) ratios, i.e., clay plant, urban incinerators, fumes from landfill and tobacco smoke, which also could be important. Finally, fresh emissions seemed to characterize the air at the sampling site, as resulting from the BaP/BeP ratio rates.

Principal components analysis (PCA) Principal component analysis (PCA), a multivariate statistical method, has applied to identify emission sources and carried out with the statistical software R. The resulting loads and percentages of variance calculated for each of the components are shown in Table 8.

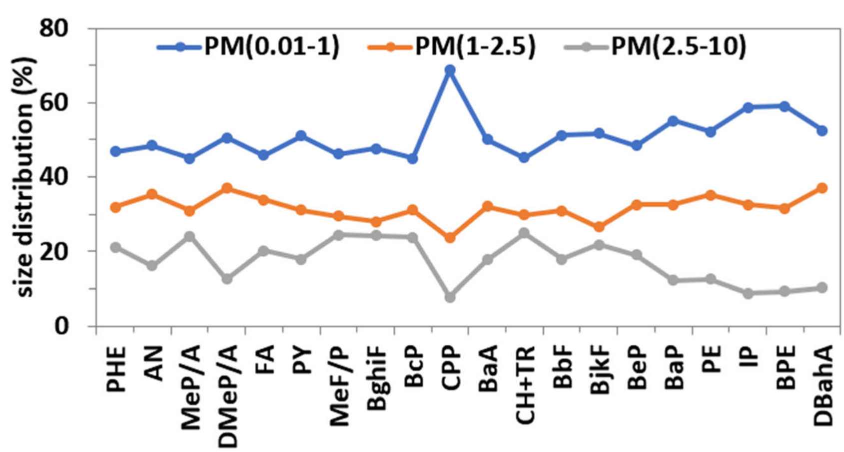

Fig. 9 PAH size distribution (%)

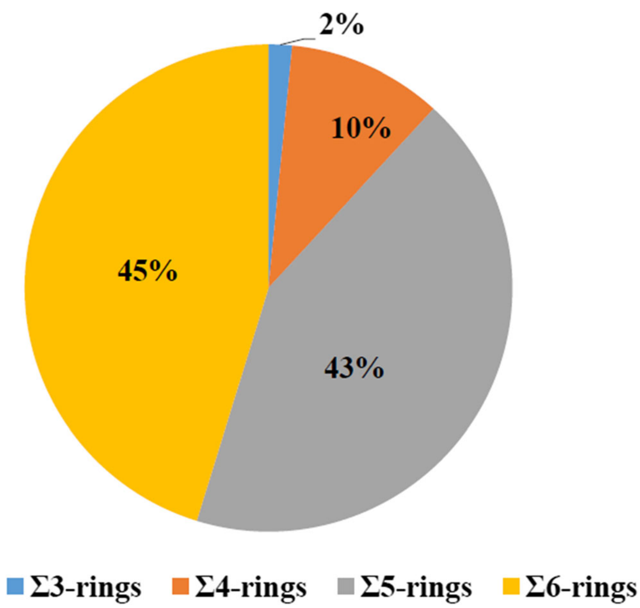

Fig. 10 PAHs ring number distribution in PM10

Only those variables with a factor load higher than 0.5 have considered in order to characterize the source of pollution.

Two components have identified in PM_1, $PM_{2.5}$, and PM_{10}, which probably represented vehicle emissions categories and stationary combustion sources.

The major components (PC1) and (PC2), respectively, accounted for 88% and 5.4% of the total variance for PM_1, 92.8% and 3.7% for $PM_{2.5}$, and 91.6% and 3.9% for PM_{10}.

The high loading factors of FA, PY, BbF, BjkF, BeP, BaP, BaA, IP, and CH for Factor 1 in all fractions confirmed that vehicle emissions were one of the main sources of PAHs.

For Factor 2, only AN had the loading factor >0.50 in PM_1, suggesting that this compound was linked to sources other than vehicles. AN had been found in coal combustion, wood combustion, and coke production by several studies (Guo et al. 2003; He et al. 2014).

All fractions of PM-bound PAHs in Bab Ezzouar city were mainly affected by vehicle exhaust and coal/coke sources.

Health risk assessment

PAHs associated with particulate matter have diverse harmful effects on human health. To assess the potential health risks of inhalation associated with human exposure to PAHs, two approaches have applied, i.e., calculation of aerial concentration of benzo[a]pyrene equivalents ([BaPeq]) and of the incremental lifetime cancer risk (ILCR) rate associated to PAHs.

Taking in account not only BaP, BaPeq was estimated as reliable to parameterize carcinogenicity associated to PAHs and is frequently applied as an indicator of human exposure to PAHs (WHO). For this purpose, neat carcinogenicity of every PAH calculated in this study was expressed in toxic equivalents relative to benzo[a]pyrene; the PAH concentrations were converted into [BaPeq] and summed using the following relationship:

Table 7 PAH diagnostic ratio

Sources	PAH ratio	FA/PY	IP/BPE	BaP/BPE	BaP/BeP	Reference
Vehicles	Mixed	0.60		0.55		Ravindra et al. 2008; Rotatori et al. 2005
	leaded gasoline	0.50	0.37	0.45	0.95	Bourotte et al. 2005; Ravindra et al. 2008; Rogge et al. 1993; Rotatori et al. 2005
	unleaded gasoline	0.54	0.2~0.35	0.35	0.95	Bourotte et al. 2005; Ravindra et al. 2008; Rogge et al. 1993; Rotatori et al. 2005
	diesel	0.8~1.1	0.65~1.1	0.8~1.1	0.50	Bourotte et al. 2005; Ravindra et al. 2008; Rogge et al. 1993; Rotatori et al. 2005; Salzano et al. 2008
Domestic heating	coal		0.9~1.3	1.57	2.10	Cecinato et al. 2005
	wood, pine	0.18	1.1~1.6	1.94	1.77	Schmidl et al. 2008
	wood, oak	0.15	1.2~1.6	1.77	0.52	Schmidl et al. 2008
	synthetic fuel	1.19	1.10	1.91		Cecinato et al. 2005
	heavy oil	0.83	1.61	0.81		Cecinato et al. 2005
Iron/steel plant)	coke (coal)	0.30	1.21	0.78	1.65	Cecinato et al. 2005 and Yang et al. 1998
	power plant (coal)	0.66	2.01	0.88	2.57	Cecinato et al. 2005 and Yang et al. 1998
Tobacco smoke	particulate	0.96	0.18	0.23	0.38	Lu and Zhu 2007
Landfill	fumes	1.30	0.76	0.70	0.55	Cecinato et al. 2005
Clay plant	fumes	~2.65	1.82	0.14	0.02	Cecinato et al. 2005
Urban incinerator	fumes	~17	0.92	~0.12	0.01	Bourotte et al. 2005; Cecinato et al. 2005; Salzano et al. 2008
This study	PM_{10}	0.90	0.48	0.14	0.37	

Table 8 PCA analysis of PAHs in PM_1, $PM_{2.5}$, and PM_{10}

PAHs	PM_1		$PM_{2.5}$		PM_{10}	
	Factor1	Fartor2	Factor1	Fartor2	Factor1	Fartor2
PHE	0.831	-	0.850	0.475	0.807	0.561
AN	-	0.814	0.975	-	0.970	-
FA	0.977	-	0.977	-	0.974	-
PY	0.976	-	0.983	-	0.978	-
CH	0.977	-	0.982	-	0.985	-
BbF	0.997	-	0.990	-	0.993	-
BjkF	0.997	-	0.992	-	0.995	-
BeP	0.928	-	0.909	-	0.928	-
BaP	0.994	-	0.994	-	0.994	-
PE	0.995	-	0.989	-	0.993	-
IP	0.979	-	0.992	-	0.988	-
DBahA	0.981	-	0.977	-	0.976	-
Eigen value	17.62	1.08	18.58	0.76	18.34	0.79
% of variance	88.08	5.41	92.89	3.78	91.69	3.94
Cumulative %	88.08	93.50	92.89	96.67	91.69	95.63
Source	Source Vehicular emission	Stationary combustion source	Source Vehicular emission	Stationary combustion source	Source Vehicular emission	Stationary combustion source

$$\text{Total BaPeq} = \sum C_i \times \text{TEF}_i$$

where $C_i$is the concentration of each *i*-PAH, and TEF_i is the corresponding toxic equivalency factor. In this study, the values established in the literature for the PAH TEFs have used (Lagoy and Nisbet 1992). The BaPeq for individual PAHs and total BaPeq for 13 PAHs have reported in Table 9.

The average of BaPeq in PM_1 was twice that in $PM_{2.5}$ and PM_{10}; the association of PM_1 with carcinogenic PAHs raises the harmful impact on humans due to the capacity of these submicronic particles to settle in the lungs.

Table 9 [BaPE] and toxic equivalency factor for total PAHs and seven carcinogenic PAHs

Compound	Toxic equivalency factor(Lagoy and Nisbet 1992)	Toxic equivalency quotients TEQ		
		PM_1	$PM_{2.5}$	PM_{10}
PHE	0.001	0.000302	0.00013	0.000162
AN	0.01	0.000437	0.000146	0.000173
FA	0.001	0.000264	0.000124	0.00015
PY	0.001	0.000339	0.000146	0.000174
CPP	0.1	0.028746	0.010849	0.011753
BaA	0.1	0.040979	0.018752	0.022965
CH	0.01	0.01042	0.004697	0.006198
BbF	0.1	0.205094	0.08865	0.107209
BjkF	0.1	0.234589	0.097616	0.12288
BaP	1	1.262647	0.561011	0.638223
IP	0.1	0.387053	0.16484	0.17846
BPE	0.01	0.078815	0.032496	0.035389
DBahA	1	0.527328	0.251108	0.275204
Total BaPE		**2.78**	**1.23**	**1.40**

Table 10 Risk parameters for different age groups

	Symbol	Units	Infants	Children	Adults
Age		Year	0–1	2–18	19–70
Body weight	BW	kg	9.1	29.7	71.05
Inhalation rate	IR	m^3/day	5.36	11.41	15.73
Exposure Frequency	EF	Days/year	350	350	350
Exposure duration	ED	Year	0–1	0–17	0–52
Averaging time	AT	Days	25550	25550	25550

BaPeq values in Bab Ezzouar were similar to those recorded in Algiers (Yassaa et al. 2001c) and higher than those reported in Bizerte (Barhoumi et al. 2018) and Naples (Di Vaio et al. 2016).

The ILCR has measured by multiplication of the lifetime average daily dose (LADD) by the slope factor BaP. The lifetime has divided into three periods as follows: infants (0–1 year), children (2–18 years), and adults (19–70 years). The global LADD has computed by summation of the LADD values of the three age groups. The following equations have used to estimate LADD and ILCR:

$$\mathrm{LADD} = \frac{\mathrm{C} \times \mathrm{EF} \times \mathrm{ED} \times \mathrm{IR}}{\mathrm{AT} \times \mathrm{BW}}$$

$$\mathrm{ILRC} = \mathrm{LADD} \times \left\{ \mathrm{CSF} \times \left(\frac{\mathrm{BW}}{70} \right)^{\frac{1}{3}} \right\} \times \mathrm{cf}$$

where:

- *C* is the concentration of [BaPeq] in air (ng m^{-3}),
- *EF* is the exposure frequency (day $year^{-1}$),
- *ED* is the exposure duration (years),
- *IR* is the air inhalation rate ($m^3 day^{-1}$),
- *AT* is the average lifetime of carcinogens (days),
- *BW* is the body weight (kg),
- *CSF* is the cancer slope factor (mg kg^{-1} day^{-1}), and
- *cf* is the conversion factor (10^{-6}) (Moya et al. 2011).

Table 10 presents the selected parameters chosen for the calculation of ILRC. The CSFs of B[a]P for the inhalation pathway have taken from the published literature (CSF = 3.14 mg kg^{-1} day^{-1}) (Hoseini et al. 2016). Residents have estimated as exposed 350 days a year during their life span.

The mean ILRC was 2×10^{-6}, 8.87×10^{-7}, and 10^{-6} for PM_1, $PM_{2.5}$, and PM_{10}, respectively. The results obtained did not exceed the tolerable level fixed by USEPA of 10^{-6} for the general population for $PM_{2.5}$ and PM_{10}, and so the risk to human health was therefore low for the citizens of Bab Ezzouar. The ILRC for PM_1 is twice as high as the USEPA tolerable level of $10^{-6.}$

Conclusion

Twenty polycyclic aromatic hydrocarbons in PM_1, $PM_{2.5}$, and PM_{10} were identified and quantified at an urban site in Bab Ezzouar city (Algeria), to draw information about their abundance in the atmosphere and distribution among PM size fractions, which influences the carcinogenic risk for humans. SEM and RaS analyses revealed that most particles were carbonaceous. The annual average concentrations of particulate matter of different sizes exceeded by far the guidelines set forth by the WHO (10 μg m^{-3}) and EU (25 μg m^{-3}) for $PM_{2.5}$ and by more than four times and twice those of the WHO (20 μg m^{-3}) and EU (40 μg m^{-3}) for PM_{10}. In addition, the annual mean concentration of PM_1 (31.1± 6.4 μg m^{-3}) recorded at the sampling site was very high and seemed to present a serious risk, regardless of their potential chemical toxicity, hence the need to introduce some regulation in national normative. Wide seasonal variations were observed of PAH concentrations in the three fractions of particulate matter, all peaking during the winter. Diagnostic ratios and PCA indicate that vehicular emissions with diesel fuel were the predominant source of PAHs. Additional sources from landfills, clay plants, and tobacco smoke were not negligible.

Though the ILCR from exposure to airborne BaPeq seemed negligible for the coarse and the fine particulates, it was important when ultrafine particles and cumulative particulates were considered. Hence, the carcinogenic risk for population residing in the study area was important. These results will contribute to the elaboration and implementation of appropriate pollution mitigation actions in Bab Ezzouar city by the political decision-makers.

Acknowledgements The authors would like to thank the medical-social center of the Civil Protection at Bab Ezzouar City for the opportunity and support provided to collect the samples needed for this study.

This work was also supported by DGRSDT (Direction Générale de la Recherche Scientifique et du Développement Technologique, Algeria).

Declarations

Competing interests The authors declare no competing interests.

References

Agudelo-Castañeda D, Teixeira EC (2014) Seasonal changes , identification and source apportionment of PAH in PM1.0. Atmos Environ 96:186–200. https://doi.org/10.1016/j.atmosenv.2014.07.030

Amil N, Latif MT, Khan MF, Mohamad M (2016) Seasonal variability of PM2.5 composition and sources in the Klang Valley urban-industrial environment. Atmos Chem Phys 16:5357–5381. https://doi.org/10.5194/acp-16-5357-2016

Barhoumi B, Castro-Jiménez J, Guigue C, Goutx M, Sempéré R, Derouiche A, Achour A, Touil S, Driss MR, Tedetti M (2018) Levels and risk assessment of hydrocarbons and organochlorines in aerosols from a North African coastal city (Bizerte, Tunisia). Environ Pollut 240:422–431. https://doi.org/10.1016/j.envpol.2018.04.109

Bharti SK, Kumar D, Anand S, Poonam, Barman SC, Kumar N (2017) Characterization and morphological analysis of individual aerosol of PM10 in urban area of Lucknow, India. Micron. 103:90–98. https://doi.org/10.1016/j.micron.2017.09.004

Bourotte C, Forti M, Taniguchi S et al (2005) A wintertime study of PAHs in fine and coarse aerosols in Sao Paulo city, Brazil. Atmos Environ 39:3799–3811. https://doi.org/10.1016/j.atmosenv.2005.02.054

Cautreels W, Van Cauwenberghe K (1976) Determination of organic compounds in airborne particulate matter by gas chromatography-mass spectrometry. Atmos Environ 10:447–457. https://doi.org/10.1016/0004-6981(76)90025-1

Cecinato A, Mabilia R, Tomasi Scianò MC, Brachetti A (2005) Benzene, idrocarburi policiclici aromatici e polveri sottili', in Minoia. New Press Publ, Como, pp 53–62

Cecinato A, Guerriero E, Balducci C, Muto V (2014) Use of the PAH fingerprints for identifying pollution sources. Urban Clim 10:630–643

Chen R, Yin P, Meng X, Liu C, Wang L, Xu X, Ross JA, Tse LA, Zhao Z, Kan H, Zhou M (2017) Fine particulate air pollution and daily mortality: A nationwide analysis in 272 Chinese cities. Am J Respir Crit Care Med 196:73–81. https://doi.org/10.1164/rccm.201609-1862OC

Cong Z, Kang S, Dong S, Liu X, Qin D (2010) Elemental and individual particle analysis of atmospheric aerosols from high Himalayas. Environ Monit Assess 160:323–335. https://doi.org/10.1007/s10661-008-0698-3

Deng L, Qian J, Liao R, Tong H (2012) Pollution characteristics of atmospheric particulates in chengdu from August to September in 2009 and their relationship with meteorological conditions. China Environ Sci 32:1433–1438

Di Vaio P, Cocozziello B, Corvino A et al (2016) Level, potential sources of polycyclic aromatic hydrocarbons (PAHs) in particulate matter (PM 10) in Naples. Atmos Environ 129:186–196. https://doi.org/10.1016/j.atmosenv.2016.01.020

Durant JL, Busby WF, Lafleur AL et al (1996) Human cell mutagenicity of oxygenated, nitrated and unsubstituted polycyclic aromatic hydrocarbons associated with urban aerosols. Mutat Res - Genet Toxicol 371:123–157. https://doi.org/10.1016/S0165-1218(96)90103-2

Eisenberg WC (1978) Fractionation of organic material extracted from suspended air particulate matter using high pressure liquid chromatography. J Chromatogr Sci 16:145–151. https://doi.org/10.1093/chromsci/16.4.145

European Union (2008) Directive 2008/50/EC of the European Parliament and of the Council of 21 May 2008 on ambient air quality and cleaner air for Europe. Official Journal of the European Union, 11 June 2008

Franzin BT, Guizellini FC, de Babos DV, Hojo O, Pastre IA, Marchi MRR, Fertonani FL, Oliveira CMRR (2020) Characterization of atmospheric aerosol (PM10 and PM2.5) from a medium sized city in São Paulo state, Brazil. J Environ Sci (China) 89:238–251. https://doi.org/10.1016/j.jes.2019.09.014

Gadi R, Sharma SK, Mandal TK et al (2018) Levels and sources of organic compounds in fine ambient aerosols over National Capital Region of India. Environ Sci Pollut Res 25:31071–31090

Gadi R, Shivani SSK, Mandal TK (2019) Source apportionment and health risk assessment of organic constituents in fine ambient aerosols (PM2.5): A complete year study over National Capital Region of India. Chemosphere 221:583–596. https://doi.org/10.1016/j.chemosphere.2019.01.067

Guo H, Lee SC, Ho KF et al (2003) Particle-associated polycyclic aromatic hydrocarbons in urban air of Hong Kong. Atmos Environ 37:5307–5317. https://doi.org/10.1016/j.atmosenv.2003.09.011

He J, Fan S, Meng Q, Sun Y, Zhang J, Zu F (2014) Polycyclic aromatic hydrocarbons (PAHs) associated with fine particulate matters in Nanjing, China: Distributions, sources and meteorological influences. Atmos Environ 89:207–215. https://doi.org/10.1016/j.atmosenv.2014.02.042

Hoseini M, Yunesian M, Nabizadeh R, Yaghmaeian K, Ahmadkhaniha R, Rastkari N, Parmy S, Faridi S, Rafiee A, Naddafi K (2016) Characterization and risk assessment of polycyclic aromatic hydrocarbons (PAHs) in urban atmospheric Particulate of Tehran, Iran. Environ Sci Pollut Res 23:1820–1832. https://doi.org/10.1007/s11356-015-5355-0

Huda MN, Hossain SA, Islam M, Islam F (2018) Chemical and Morphological Characteristics of Particulate Matter Suspended in the Air of the Dhaka University Area of Bangladesh. Air Pollut 7:95–106. https://doi.org/10.4236/ojap.2018.72005

Jamhari AA, Sahani M, Latif MT, Chan KM, Tan HS, Khan MF, Mohd Tahir N (2014) Concentration and source identification of polycyclic aromatic hydrocarbons (PAHs) in PM10 of urban, industrial and semi-urban areas in Malaysia. Atmos Environ 86:16–27. https://doi.org/10.1016/j.atmosenv.2013.12.019

Jodeh S, Hasan AR, Amarah J, Judeh F, Salghi R, Lgaz H, Jodeh W (2018) Indoor and outdoor air quality analysis for the city of Nablus in Palestine: seasonal trends of PM10, PM5.0, PM2.5, and PM1.0 of residential homes. Air Qual Atmos Health 11:229–237. https://doi.org/10.1007/s11869-017-0533-5

Kadowaki S (1994) Characterization of Carbonaceous Aerosols in the Nagoya Urban Area . 2 . Behavior and Origin of Particulate n-Alkanes. Environ Sci Technol 28:129–135

Kalisa E, Nagato EG, Bizuru E, Lee KC, Tang N, Pointing SB, Hayakawa K, Archer SDJ, Lacap-Bugler DC (2018) Characterization and Risk Assessment of Atmospheric PM2.5 and PM10 Particulate-Bound PAHs and NPAHs in Rwanda, Central-East Africa. Environ Sci Technol 52:12179–12187. https://doi.org/10.1021/acs.est.8b03219

Kerchich Y, Yacine M, Kerbachi R (2016) Atmospheric levels of BTEXs, PM2.5, PM10 and heavy metals at Algiers city. Fresenius Environ Bull 25:2519–2530

Khairy MA, Lohmann R (2013) Chemosphere Source apportionment and risk assessment of polycyclic aromatic hydrocarbons in the atmospheric environment of Alexandria , Egypt. Chemosphere 91:895–903. https://doi.org/10.1016/j.chemosphere.2013.02.018

Khedidji S, Balducci C, Ladji R, Cecinato A, Perilli M, Yassaa N (2017) Chemical composition of particulate organic matter at industrial, university and forest areas located in Bouira province, Algeria. Atmos Pollut Res 8:474–482. https://doi.org/10.1016/j.apr.2016.12.005

Kozáková J, Leoni C, Klán M et al (2018) Chemical Characterization of PM1-2.5 and its Associations with PM1, PM2.5-10 and Meteorology in Urban and Suburban Environments. Aerosol Air Qual Res 18:1684–1697. https://doi.org/10.4209/aaqr.2017.11.0479

Krumal K, Mikuska P, Vecera Z (2013) Polycyclic aromatic hydrocarbons and hopanes in PM1 aerosols in urban areas r. Atmos Environ 67:27–37. https://doi.org/10.1016/j.atmosenv.2012.10.033

Ladji R, Yassaa N, Balducci C, Cecinato A, Meklati BY (2009a) Annual variation of particulate organic compounds in PM 10 in the urban atmosphere of Algiers. Atmos Res 92:258–269. https://doi.org/10.1016/j.atmosres.2008.12.002

Ladji R, Yassaa N, Balducci C, Cecinato A, Meklati BY (2009b) Science of the Total Environment Distribution of the solvent-extractable organic compounds in fi ne (PM 1) and coarse (PM 1 – 10) particles in urban , industrial and forest atmospheres of Northern

Algeria. Sci Total Environ 408:415–424. https://doi.org/10.1016/j.scitotenv.2009.09.033

Lagoy PK, Nisbet ICT (1992) Toxic Equivalency Factors (TEFs) for Polycyclic Aromatic Hydrocarbons (PAHs). Regul Toxicol Pharmacol 16:290–300

Landkocz Y, Ledoux F, André V, Cazier F, Genevray P, Dewaele D, Martin PJ, Lepers C, Verdin A, Courcot L, Boushina S, Sichel F, Gualtieri M, Shirali P, Courcot D, Billet S (2017) Fine and ultrafine atmospheric particulate matter at a multi-influenced urban site: Physicochemical characterization, mutagenicity and cytotoxicity. Environ Pollut 221:130–140. https://doi.org/10.1016/j.envpol.2016.11.054

Lu H, Zhu L (2007) Pollution patterns of polycyclic aromatic hydrocarbons in tobacco smoke. J Hazard Mater 139:193–198. https://doi.org/10.1016/j.jhazmat.2006.06.011

Mahato S, Pal S, Ghosh KG (2020) Effect of lockdown amid COVID-19 pandemic on air quality of the megacity Delhi , India. Sci Total Environ 730:139086. https://doi.org/10.1016/j.scitotenv.2020.139086

Manoli E, Kouras A, Karagkiozidou O, Argyropoulos G, Voutsa D, Samara C (2015) Polycyclic aromatic hydrocarbons (PAHs) at traffic and urban background sites of northern Greece : source apportionment of ambient PAH levels and PAH-induced lung cancer risk. Environ Sci Pollut Res 23:3556–3568. https://doi.org/10.1007/s11356-015-5573-5

Moussaoui Y, Balducci C, Cecinato A, Meklati BY (2010) Chemical composition of extractable organic matter of airborne particles in urban and rural atmospheres of northern Algeria. Fresenius Environ Bull 19:2497–2508

Moussaoui Y, Balducci C, Cecinato A, Meklati BY (2013a) Urban Climate Atmospheric particulate organic matter at urban and forest sites of Northern Algeria. Urban Clim 4:85–101. https://doi.org/10.1016/j.uclim.2013.05.001

Moussaoui Y, Boumechhour A, Jaffrezo JL, Meklati BY (2013b) The chemical composition of inorganic and carbonaceous materials in PM 10 from urban and rural Algerian areas. Fresenius Environ Bull 22:1357–1366

Moya J, Laurie S, Phillips L, et al (2011) Exposure factors handbook. In: Edition 11 (ed) US Environmental Protection Agency, Washington

Mukherji S, Swain AK, Venkataraman C (2002) Comparative mutagenicity assessment of aerosols in emissions from biofuel combustion. Atmos Environ 36:5627–5635. https://doi.org/10.1016/S1352-2310(02)00690-8

NOM (2019) National Office of Meteorology in Algiers. http://www.meteo.dz. Accessed 18 march 2019

NOS (2008) Algeria. http://www.ons.dz. Accessed 20 Jan 2020

Oucher N, Kerbachi R (2012) Evaluation of Air Pollution by Aerosol Particles Due to Road Traffic : A Case Study from Algeria. Procedia Eng 33:415–423. https://doi.org/10.1016/j.proeng.2012.01.1221

Pateraki S, Fameli K, Assimakopoulos V et al (2019) Levels , Sources and Health Risk of PM 2 . 5 and PM 1-Bound PAHs across the Greater Athens Area : The Role of the Type of Environment and the Meteorology. Atmosphere (Basel) 10:622–640

Ravindra K, Sokhi R, Van Grieken R (2008) Atmospheric polycyclic aromatic hydrocarbons : Source attribution , emission factors and regulation. Atmos Environ 42:2895–2921. https://doi.org/10.1016/j.atmosenv.2007.12.010

Rogge WF, Hlldemann LM, Mazurek MA, Cass GR (1993) Sources of Fine Organic Aerosol . 2 . Noncatalyst and Catalyst-Equipped Automobiles and Heavy-Duty Diesel Trucks. Environ Sci Technol 27:636–651

Rogula-Kozłowska W, Majewski G, Rogula-Kopiec P, Mathews B (2019) Mass concentration and chemical composition of submicron particulate matter (PM 1) in the Polish urban areas. earth. Environ Sci. https://doi.org/10.1088/1755-1315/214/1/012092

Romagnoli P, Balducci C, Perilli M, Esposito G, Cecinato A (2019) Organic molecular markers in marine aerosols over the Western Mediterranean Sea. Environ Pollut 248:145–158. https://doi.org/10.1016/j.envpol.2019.02.020

Rotatori M, Cecinato A, Sbrilli A et al (2005) Benzene, idrocarburi policiclici aromatici e polveri sottili, in Minoia. New Press Publ, Como, pp 73–82

Salzano R, Mabilia R, Salvatori R et al (2008) Spectro-radiometric and PAH chemical characterization of vehicle particulate emissions at the chassis dynamometer. Fresenius Environ Bull 17:1711–1716

Schmidl C, Bauer H, Dattler A, Hitzenberger R, Weissenboeck G, Marr IL, Puxbaum H (2008) Chemical characterisation of particle emissions from burning leaves. Atmos Environ 42:9070–9079. https://doi.org/10.1016/j.atmosenv.2008.09.010

Stephanou EG, Stratigakis NE (1993) Determination of anthropogenic and biogenic organic compounds on airborne particles: flash chromatographic fractionation and capillary gas chromatographic analysis. J Chromatogr A 644:141–151. https://doi.org/10.1016/0021-9673(93)80124-Q

Talbi A, Kerchich Y, Kerbachi R (2018) Assessment of annual air pollution levels with PM1 , PM2 . 5 , PM10 and associated heavy metals in Algiers , Algeria. Environ Pollut 232:252–263. https://doi.org/10.1016/j.envpol.2017.09.041

Terrouche A, Ali-khodja H (2015) Identification of sources of atmospheric particulate matter and trace metals in Constantine, Algeria. Air Qual Atmos Health 9:69–82. https://doi.org/10.1007/s11869-014-0308-1

USEPA-Method IO-3.1 (1999) United states environmental protection agency. Compendium of methods for the determination of inorganic compounds in ambient air; EPA/ 625/R-96/010a. Selection, preparation and extraction of filter material

WB (2017) World Bank. PM2.5 air pollution, mean annual exposure. https://data.worldbank.org/indicator/EN.ATM.PM25.M. Accessed 18 Jan 2020

WHO (2014) Air Pollution Ranking. https://aqicn.org/faq/2015-05-16/world-health-organization-2014-air-pollution-ranking/. Accessed 22 Jan 2020

Yang H, Lee W, Chen S, Lai S-O (1998) PAH emission from various industrial stacks. J Hazard Mater 60:159–174

Yassaa N, Meklati BY, Cecinato A (2001a) Chemical characteristics of organic aerosols in Algiers city area: Influence of a fat manufacture plant. Atmos Environ 35:6003–6013. https://doi.org/10.1016/S1352-2310(01)00366-1

Yassaa N, Meklati BY, Cecinato A, Marino F (2001b) Particulate n -alkanes , n -alkanoic acids and polycyclic aromatic hydrocarbons in the atmosphere of Algiers City Area. Atmos Environ 35:1843–1851

Yassaa N, Meklati BY, Cecinato A, Marino F (2001c) Organic aerosols in urban and waste landfill of Algiers metropolitan area: Occurrence and sources. Environ Sci Technol 35:306–311. https://doi.org/10.1021/es991316d

Yassaa N, Meklati BY, Cecinato A, Marino F (2001d) Chemical characteristics of organic aerosol in Bab-Ezzouar (Algiers). Contribution of bituminous product manufacture. Chemosphere 45:315–322. https://doi.org/10.1016/S0045-6535(00)00566-X

Zahran AA, Ibrahim MI, Ramadan AE-D, Ibrahim MM (2018) Air Quality Indices, Sources and Impact on Human Health of PM10 and PM2.5 in Alexandria Governorate, Egypt. J Environ Protect (Irvine, Calif) 09:1237–1261. https://doi.org/10.4236/jep.2018.912078

Publisher's note Springer Nature remains neutral with regard to jurisdictional claims in published maps and institutional affiliations.